Supporting Information for

Color-tuning lanthanide metal-organic framework gels

Fei Chen,[a] Yong-Mei Wang,[a] Weiwei Guo,[a] Xue-Bo Yin[a,b,*]

[a]State Key Laboratory of Medicinal Chemical Biology and Tianjin Key Laboratory of Biosensing and Molecular Recognition, College of Chemistry, Nankai University, Tianjin, 300071, China

[b]Collaborative Innovation Center of Chemical Science and Engineering (Tianjin), Nankai University, Tianjin, 300071, China

*Correspondence: xbyin@nankai.edu.cn; Fax: +86-22-23503034

1. Experimental Procedures

1.1 Materials

Europium(III) chloride hexahydrate ($EuCl_3 \cdot 6H_2O$), terbium(III) chloride hexahydrate ($TbCl_3 \cdot 6H_2O$), and dysprosium(III) chloride hexahydrate ($DyCl_3 \cdot 6H_2O$) was obtained from Sigma−Aldrich, Shanghai, China. N, N-dimethylformamide (DMF) was obtained from Tianjin chemical reagent Co., Ltd., Tianjin, China. Isophthalic acid (isp) was obtained from Shanghai Macklin Biochemical Co.,Ltd. 5-boronoisophthalicacid (5-bop) was purchased from HWRK Chemicals Co., Ltd. (Beijing, China). [1,1'-Biphenyl]-3,5-dicarboxylic acid was obtained from Chemsoon, Shanghai, China. 5-Hydroxyisophthalic acid was obtained from TCLchemicals, Shanghai, China. 5-Aminoisophthalic acid was from Shanghai Macklin Biochemical Co., Ltd. Ferric chloride, ferrous chloride, aluminium chloride, lead chloride, potassium dichromate, sodium fluoride obtained from Municipality kemi'ou Chemical Reagent Co. (Tianjin, China). All the chemicals were obtained at least of analytical grade and used without further purification. Ultra-pure water was prepared with an Aquapro system (18.25 MΩ cm).

1.2 Instrument and Characterization

Transmission electron microscopy (TEM) images were recorded with Tecnai G2 F20, FEI Co., America operated at an accelerating voltage of 200 kV. Scanning electron microscopy (SEM) images were recorded with JSM-7500F, Japan. The steady-state fluorescence experiments were performed on a FL-4600 fluorescence spectrometer (Hitachi, Japan) equipped with a plotter unit and a quartz cell (1 cm×1 cm). X-ray photoelectron spectroscopy (XPS) analysis was performed by Kratos Axis Ultra DLD spectrometer fitted with a monochromated Al-Kα X-ray source (1486.6 eV), hybrid (magnetic/electrostatic) optics, and a multi-channel plate and delay line detector. X-ray diffraction (XRD) patterns were recorder on a D/max-2500 diffractometer (Rigaku, Japan) using Cu-K α radiation (λ = 1.5418 Å). For the record of their powder XRD, the MOF gels were dried to obtain solid products. The solid powers were submitted to obtain the XRD patterns of the MOF gels. The infrared spectra were measured by the Bruker TENSOR 27 Fourier transform infrared spectroscopy. The content of Eu, Tb, and Dy was measured by Inductively Coupled Plasma Atomic Emission Spectroscopy (ICP-AES), IRIS advantage, Thermo, USA. Rheological

measurements were performed using an DHR-2 Rheometer (TA Instruments) equipped with a 40 mm parallel-plate geometry with a gap size of 0.5 mm. The measurement temperature was set at 25 °C. The oscillatory strain sweep measurements were performed from 0.01% to 100% strain with a fixed frequency of 1 Hz.

1.3 Synthesis of the single- or mixed-metal-organic framework

1.3.1 Synthesis of Boric-Acid-Functional MOFs of Eu –MOF 1, Tb -MOF 1 and Dy-MOF 1

Boric acid-functional Eu-MOF 1 were synthesized by simple solvothermal method. A mixture of $EuCl_3 \cdot 6H_2O$ (0.1 mmol, 36.6 mg) and 5-bop (0.1 mmol, 21.0 mg) were vigorously stirred for 5 min in 10 ml DMF/H_2O (7:3) solution. Then, the mixed solution was transferred into a 20ml bottle and heated at 120 °C for 12 h. Then the mixture was cooled to room temperature. Tb-MOF 1 and Dy-MOF 1 were synthesized in the similar procedure as Eu-MOF, except $TbCl_3 \cdot 6H_2O$ (0.1 mmol, 37.3mg) and $DyCl_3 \cdot 6H_2O$ (0.1 mmol, 37.7 mg) were used as the metal sources, respectively.

1.3.2 Synthesis of Boric-Acid-Functional MOFs of Eu-Tb-MOF, Eu-Dy-MOF, Tb-Dy-MOF and Eu-Tb-Dy-MOF

Boric acid-functional Eu-Tb-MOF were synthesized by simple solvothermal method. A mixture of $EuCl_3 \cdot 6H_2O$ (0.05 mmol, 18.3 mg), $TbCl_3 \cdot 6H_2O$ (0.05mmol, 18.6 mg) and 5-bop (0.1 mmol, 21.0 mg) were vigorously stirred with 10 ml DMF/H_2O (7:3) solution for 5 min in a 20 ml bottle. Then, the mixed solution was heated at 120 °C for 12 h. The mixture was cooled to room temperature after reaction. Eu-Dy-MOF, Tb-Dy-MOF and Eu-Tb-Dy-MOF were synthesized in the similar procedure as Eu-Tb-MOF, except $EuCl_3 \cdot 6H_2O$ (0.05 mmol, 18.3 mg) and $DyCl_3 \cdot 6H_2O$ (0.05 mmol, 18.8 mg); $TbCl_3 \cdot 6H_2O$ (0.05 mmol,18.6 mg) and $DyCl_3 \cdot 6H_2O$ (0.05 mmol, 18.8 mg); $EuCl_3 \cdot 6H_2O$ (0.033 mmol, 12.2 mg), $TbCl_3 \cdot 6H_2O$ (0.033 mmol, 12.4 mg) and $DyCl_3 \cdot 6H_2O$ (0.033 mmol, 12.6 mg) were used as the metal sources, respectively.

1.3.3 Synthesis of Eu-MOF 2, Tb-MOF 2 and Dy-MOF 2 with the Isophthalic acid (ISP) as ligand

Eu-MOF 2 were synthesized by simple solvothermal method. A mixture of $EuCl_3 \cdot 6H_2O$ (0.1 mmol, 36.6 mg) and isp (0.1 mmol, 16.6 mg) were vigorously stirred for 5 min in 10 ml

DMF/H_2O (7:3) solution. Then, the mixed solution was transferred into a 20ml bottle and heated at 120 °C for 12 h. Then the mixture was cooled to room temperature. Tb-MOF 2 and Dy-MOF 2 were synthesized in the similar procedure as Eu-MOF, except $TbCl_3 \cdot 6H_2O$ (0.1 mmol, 37.3mg) and $DyCl_3 \cdot 6H_2O$ (0.1 mmol, 37.7 mg) were used as the metal sources, respectively.

1.3.4 Synthesis of Boric-Acid-Functional Tb-MOFs with different reaction concentrations

Boric acid-functional Tb-MOF with different concentrations were synthesized by simple solvothermal method. Mixtures of $TbCl_3 \cdot 6H_2O$ (five different reactant concentrations based on at 5, 10, 20, 30 and 40 mmol L^{-1} $TbCl_3 \cdot 6H_2O$) and 5-bop (five different reactant concentrations: 5, 10, 20, 30 and 40 mmol L^{-1} 5-bop) were respectively stirred with 10 ml DMF/H_2O (7:3) solution for 5 min in five 20 ml bottles. Then, the mixed solution was heated at 120 °C for 12 h. The mixture was cooled to room temperature after reaction.

1.3.5 Synthesis of Boric-Acid-Functional Tb-MOFs with different reaction time.

Boric-Acid- Functional Tb-MOFs with different reaction time were synthesized by simple solvothermal method. Ten mixtures with the same of $TbCl_3 \cdot 6H_2O$ (0.1 mmol, 37.3 mg) and 5-bop (0.1 mmol, 21.0 mg) were respectively stirred with 10 ml DMF/H_2O (7:3) solution for 5 min in ten 20 ml bottles. Then, the mixed solution were respectively heated at 120 °C for 1, 1.5, 2, 2.5, 3, 4, 6, 8, 10, and12 h. The mixtures were cooled to room temperature after reaction.

1.3.6 Synthesis of Eu-MOF, Tb-MOF and Dy-MOF with the [1,1'-biphenyl]-3,5-dicarboxylic acid, 5-hydroxyisophthalic acid and 5-aminoisophthalic acid as ligand,respectively.

Three kinds of Eu-MOFs were synthesized by simple solvothermal method. A mixture of $EuCl_3 \cdot 6H_2O$ (0.1 mmol, 36.6 mg) and [1,1'-biphenyl]-3,5-dicarboxylic acid (0.1 mmol, 24.2 mg), or 5-hydroxyisophthalic acid (0.1 mmol,18.2 mg), or 5-aminoisophthalic acid (0.1 mmol, 18.1 mg), respectively, were vigorously stirred for 5 min in 10 ml DMF/H_2O (7:3) solution. Then, the mixed solution was transferred into a 20ml bottle and heated at 120 °C for 12 h. Then the mixture was cooled to room temperature. Tb-MOFs and Dy-MOFs were synthesized in the similar procedure as Eu-MOFs, except $TbCl_3 \cdot 6H_2O$ (0.1 mmol, 37.3mg)

and $DyCl_3 \cdot 6H_2O$ (0.1 mmol, 37.7 mg) were used as the metal sources, respectively.

1.3.7 Luminescence Measurements for Sensing of different analytes

To explore the luminescence sensing properties of the MOF gels for detection of different analytes, the photoluminescence emission spectra of suspensions of the $Eu_{0.25}Tb_{0.25}Dy_{0.5}$-MOF gels under the single excitation of 259 nm at room temperature were recorded upon addition of a series of analytes with different concentration (F^-, Al^{3+}, Fe^{2+}, Pb^{2+} of 1, 2, 3 mmol/L, respectively; $Cr_2O_7^{2-}$ of 0.05, 0.075, 0.1 mmol/L and Fe^{3+} of 0.025, 0.05, 0.075 mmol/L).

2. Results and Discussion

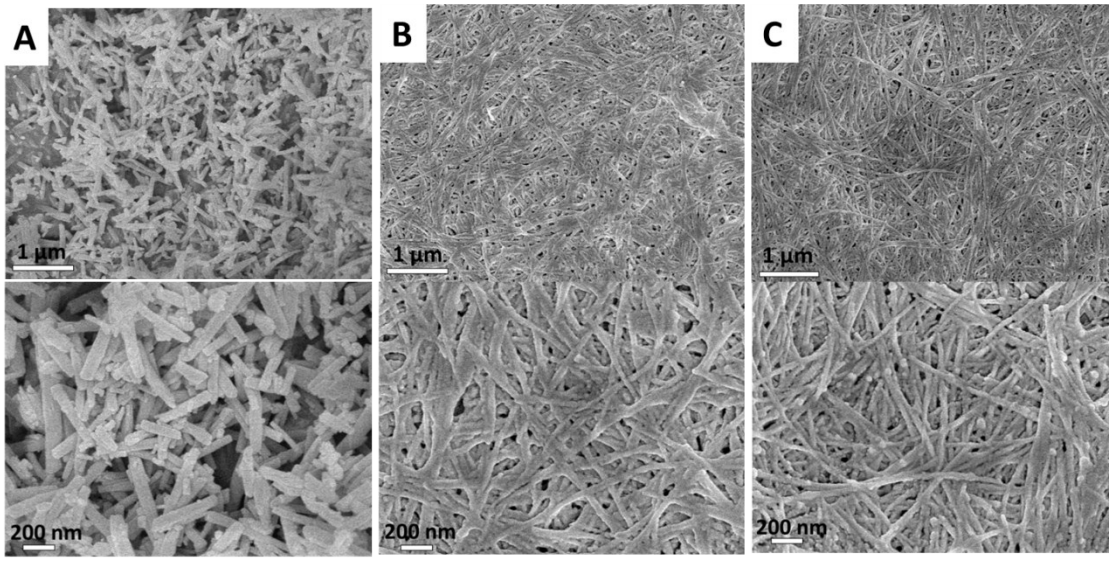

Figure S1. SEM images of the MOFs with different amplification. (A) Eu-MOFs, (B) Tb-MOFs, and (C) Dy-MOFs prepared with 5-bop as ligand and Eu^{3+}, Tb^{3+}, and Dy^{3+} ions as metal nodes under 120 °C under atmospheric pressure, respectively.

Table S1. The energy level of S_1 and T_1 of 5-bop and ISP

	S_1 (cm^{-1})	T_1 (cm^{-1})	Energy gap between T_1 and Ln^{3+} ions (cm^{-1})		
			Eu^{3+} $^5D_0$, 18674 cm^{-1}	Tb^{3+} $^5D_4$, 20500 cm^{-1}	Dy^{3+} $^4F_{2/9}$ 22000 cm^{-1}
5-bop	35335	23923	5249	3423	1923
ISP	35714	22831	4157	2331	831

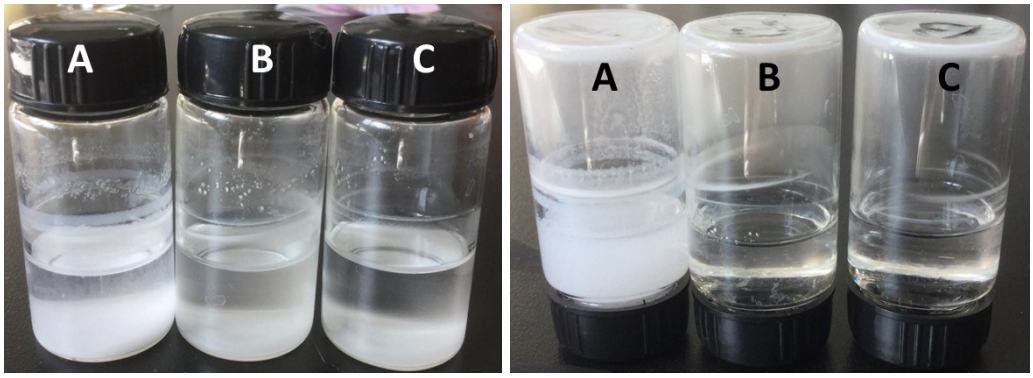

Figure S2. The photos of (A) Eu-MOFs, (B) Tb-MOFs, and (C) Dy-MOFs prepared with ISP as ligand and Eu^{3+}, Tb^{3+}, and Dy^{3+} ions as metal nodes under 120 °C under atmospheric pressure.

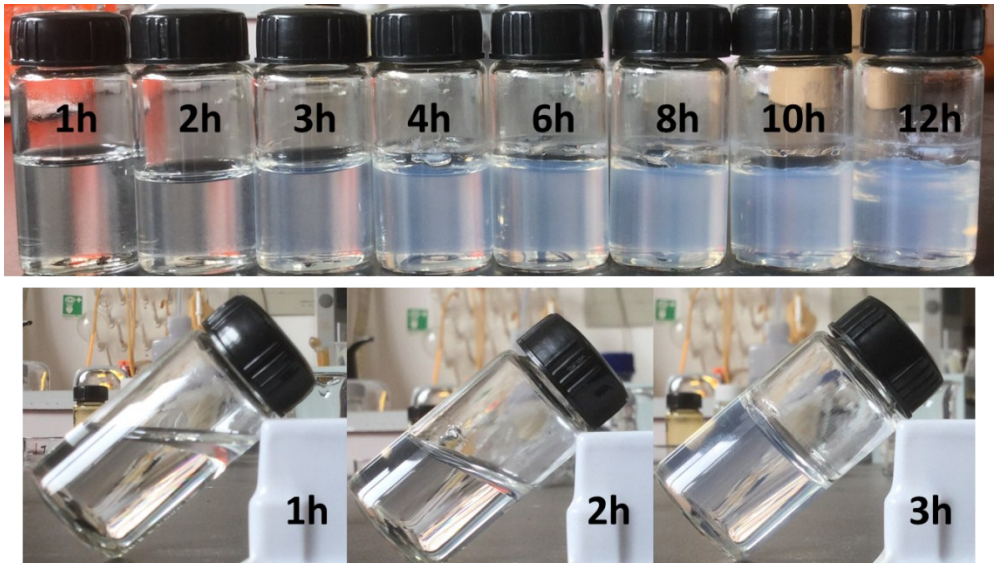

Figure S3. The photos of the Tb-MOFs with different reaction time. Tb-MOFs prepared with 5-bop as ligand and Tb^{3+} ions as metal node under 120 °C under atmospheric pressure.

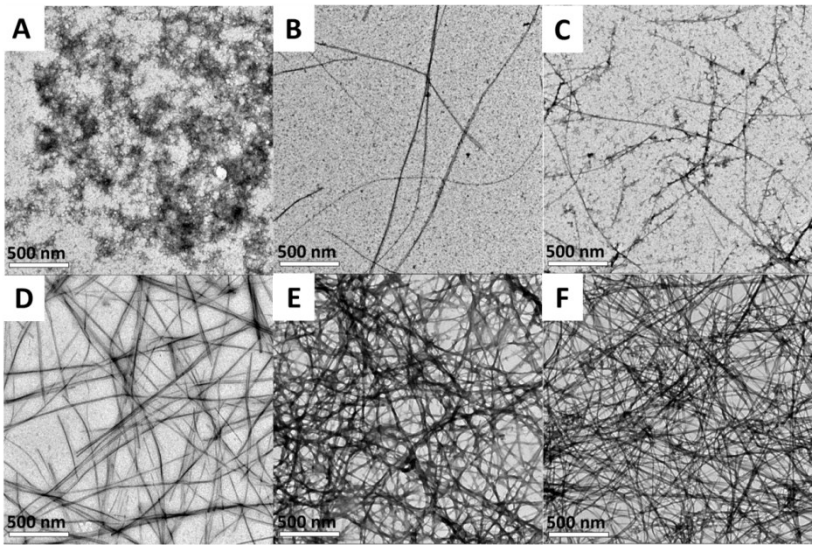

Figure S4. TEM images of Tb-MOFs with different reaction time. Tb-MOFs prepared with 5-bop as ligand and Tb^{3+} ions as metal node under 120 °C under atmospheric pressure for (A) 1, (B) 1.5, (C) 2, (D) 2.5, (E) 3, and (F) 6 h.

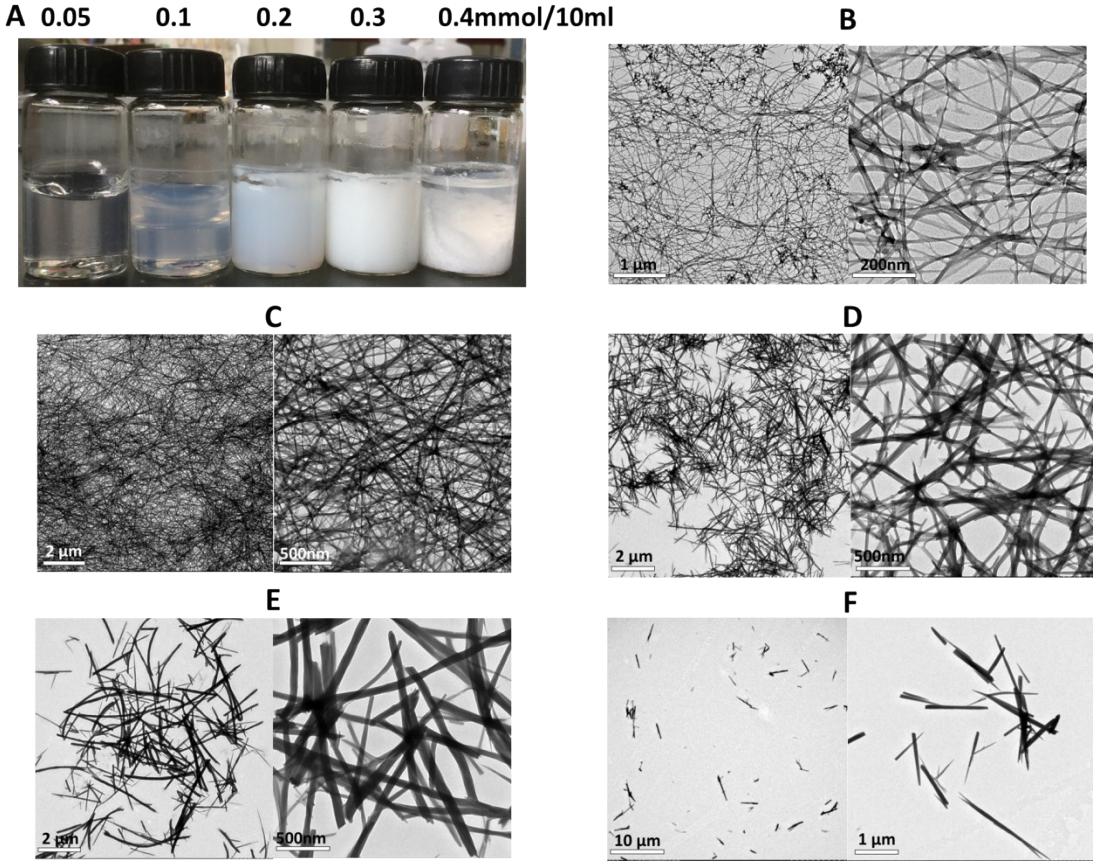

Figure S5. (A) The photos of the products with different Tb content. TEM images of the products prepared with (B) 0.05, (C) 0.1, (D) 0.2, (E) 0.3 (F) 0.4 mmol Tb^{3+} ions in 10 ml DMF/H_2O.

Table S2. Crystallographic data collection and refinement of Eu-ISP-MOFs

Compound	Eu- ISP-MOFs
Chemical formula	$C_{24}H_{16}Eu_2O_{14}$
Formula mass	832.29 g/mol
Crystal system	Monoclinic
Space group	p 21/n
Unit cell dimensions	a = 13.320(3) Å, α = 90.000°
	b = 14.481(3) Å, β = 104.377(4)°
	c = 13.459(3) Å, γ = 90.000°
Cell Volume	2514.8 (8)$Å^3$
Z	4
Temperature	113(2) K
Wavelength	0.17073 Å
Crystal size	0.12×0.18×0.2 mm^3
Calculated Density	2.19817 g/cm^{-3}
F(000)	1592.0
Absorption coefficient	5.017 mm^{-1}
R (int)	0.030
Goodness of fit on F2	1.0070
Limiting indices	-17 ≤ h ≤ 17, -18 ≤ k ≤17, -17 ≤ l7
Final R indices I>2sigma(I)	R 1a = 0.0377, wR 2b = 0.0780
R indices (all data)	R 1 = 0.0477, wR 2 = 0.0842

Table S3. Crystallographic data collection and refinement of Tb-ISP-MOFs

Compound	Tb- ISP-MOFs
Chemical formula	$C_{24}H_{18}Tb_2O_{15}$
Formula mass	864.22g/mol
Crystal system	Monoclinic
Space group	p 21/n
Unit cell dimensions	a = 10.537(2) Å, α = 90.000°
	b = 14.162(3) Å, β = 97.364(5)°
	c = 16.923(3) Å, γ = 90.000°
Cell Volume	2506.3(9)$Å^3$
Z	4
Temperature	113(2) K
Wavelength	0.71073 Å
Crystal size	0.12×0.18×0.2 mm^3
Calculated Density	2.290 g/cm^{-3}
F(000)	1648
Absorption coefficient	5.678 mm^{-1}
R (int)	0.0386
Goodness of fit on F2	0.984
Limiting indices	$-13 \leq h \leq 13$, $-18 \leq k \leq 18$, $-21 \leq 21$
Final R indices I>2sigma(I)	R 1a = 0.0175, wR 2b = 0.0368
R indices (all data)	R 1 = 0.0151, wR 2 = 0.0363

Table S4. Crystallographic data collection and refinement of Dy- ISP-MOFs

Compound	Dy- ISP-MOFs
Chemical formula	$C_{48}H_{36}Dy_4O_{30}$
Formula mass	1742.77 g/mol
Crystal system	Monoclinic
Space group	P 21/c
Unit cell dimensions	a = 10.5772(19) Å α = 90 °. b = 14.206(3) Å β = 97.363(7) °. c = 16.976(4) Å γ = 90 °.
Cell Volume	2529.7(9) $Å^3$
Z	2
Temperature	133(2) K
Wavelength	0.71073 Å
Crystal size	0.18 x 0.10 x 0.10 mm
Calculated Density	2.288 g/m^3
F(000)	1656
Absorption coefficient	5.941 mm^{-1}
R (int)	0.0293
Goodness of fit on F2	1.015
Limiting indices	$-13\leq h\leq 13$, $-18\leq k\leq 18$, $-22\leq l\leq 21$
Final R indices I>2sigma(I)	R1 = 0.0114, wR2 = 0.0285
R indices (all data)	R1 = 0.0131, wR2 = 0.0288

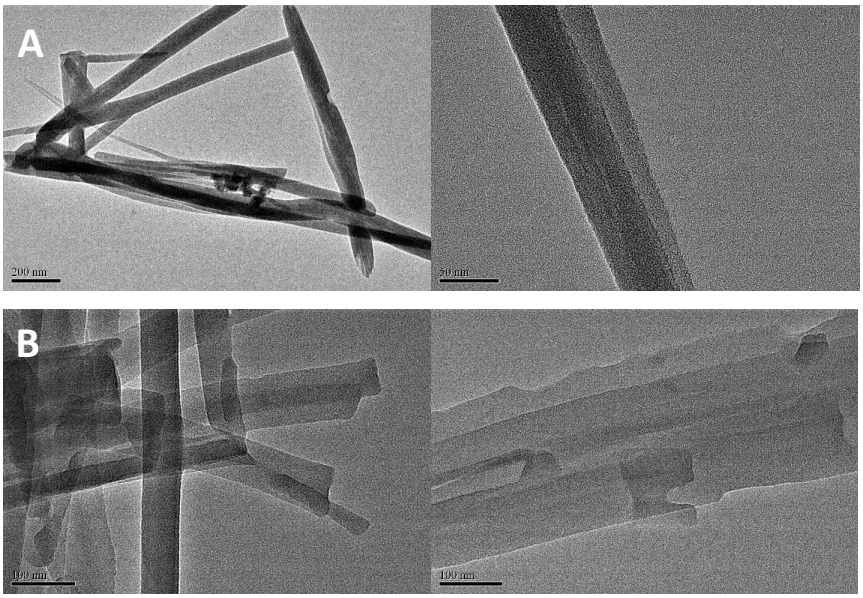

Figure S6. TEM images of (A) Eu-MOFs, and (B) Tb-MOFs with ISP as ligand.

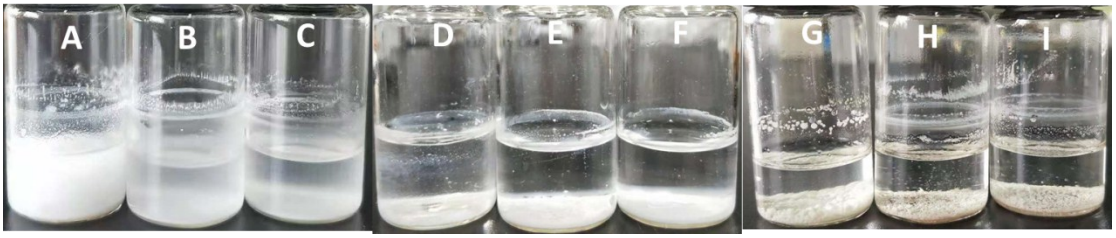

Figure S7. Photographs of (A) (D) (G) Eu-MOFs, (B) (E) (H) Tb-MOFs, and (C) (F) (I) Dy-MOFs with [1,1'-Biphenyl]-3,5-dicarboxylic acid, 5-hydroxyisophthalic acid and 5-aminoisophthalic acid as ligand, respectively.

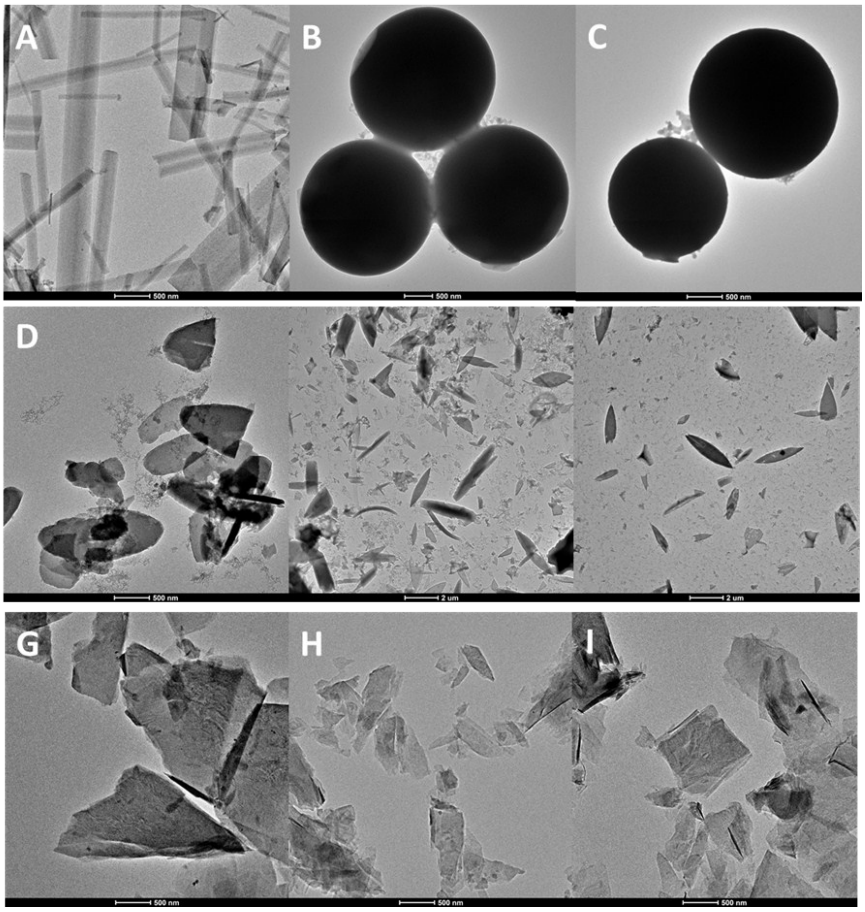

Figure S8. TEM images of (A) (D) (G) Eu-MOFs, (B) (E) (H)Tb-MOFs, and (C) (F) (I) Dy-MOFs with [1,1'-Biphenyl]-3,5-dicarboxylic acid, 5-hydroxyisophthalic acid and 5-aminoisophthalic acid as ligand, respectively.

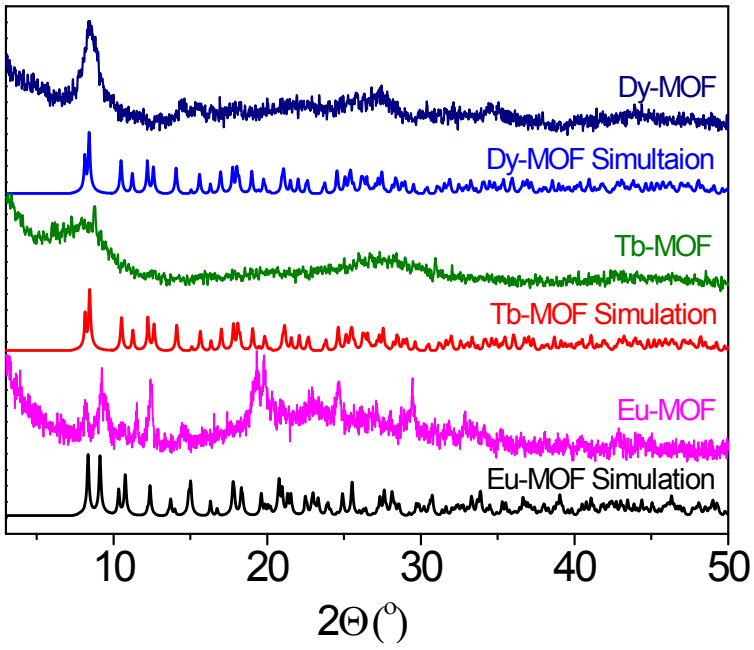

Figure S9. Powder diffraction patterns of the Ln-NMOF gels and simulation results from

single crystal of Eu-ISP MOFs, Tb-ISP MOFs, and Dy-ISP MOFs.

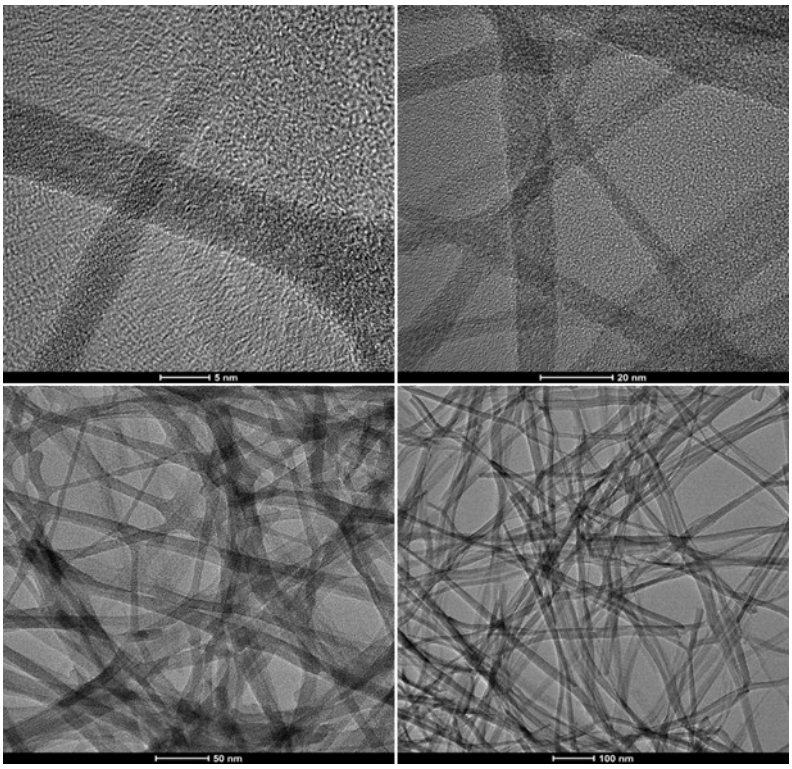

Figure S10. High magnification TEM images of Tb-MOF gels.

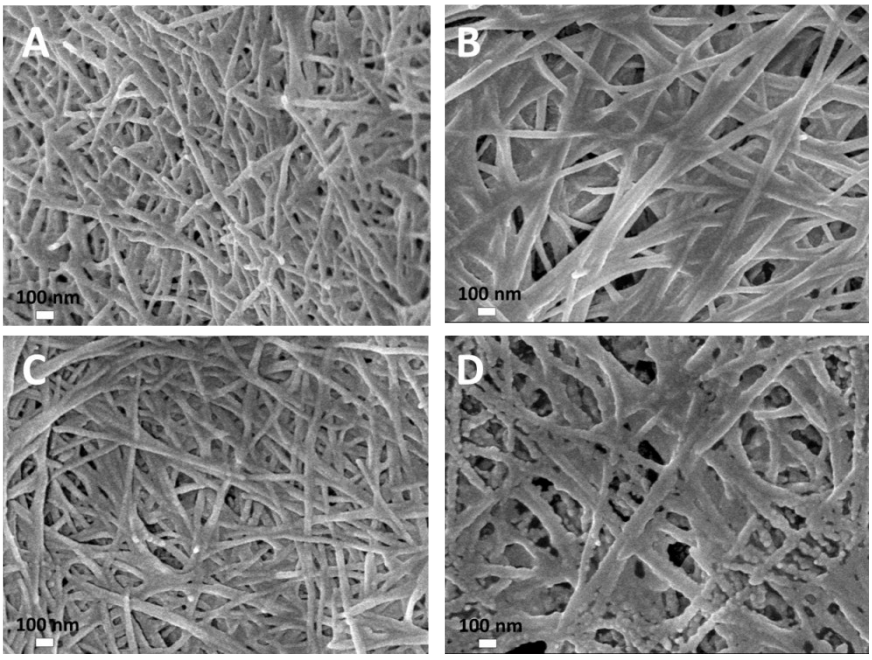

Figure S11. SEM images of (A) Eu-Tb, (B) Eu-Dy, (C) Dy-Tb, and (D) Eu-Tb-Dy MOF gels prepared with 5-bop as ligand and bi-metal or tri-metal as metal nodes with the ratio of 1:1 or 1:1:1 under 120 °C under atmospheric pressure, respectively.

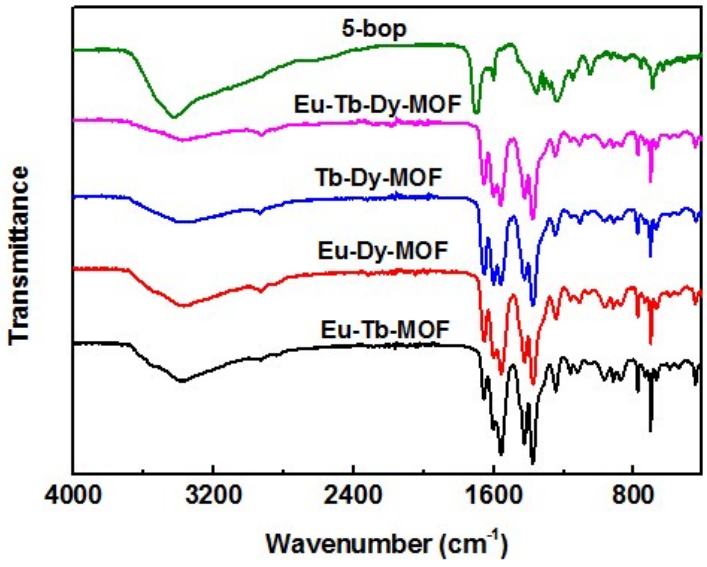

Figure S12. Fourier transform infrared spectra (FTIR) spectra of 5-bop, Eu-Tb-Dy-MOF, Tb-Dy-MOF, Eu-Dy-MOF, Eu-Tb-MOF.

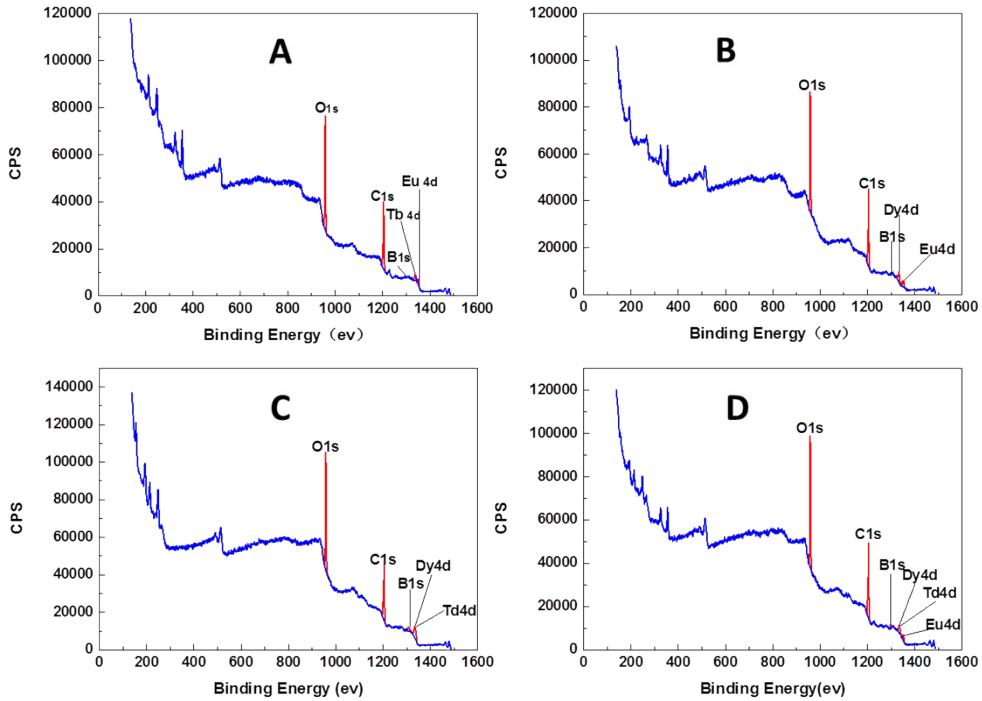

Figure S13. XPS spectra of (A) Eu-Tb-MOF gels, (B) Eu-Dy-MOF gels, (C) Tb-Dy-MOF gels, and (D) Eu-Tb-Dy-MOF gels.

Table S5. Eu/Tb/Dy molar ratios of the Eu-Tb-MOF gels (1:1), Eu-Dy-MOF gels (1:1), Tb-Dy-MOF gels (1:1), and Eu-Tb-Dy-MOF gels (1:1:1) in precursors and obtained from ICP-AES

Sample	In precursors	In ICP-AES results
Eu-Tb-MOF gel (1:1)	1:1	1:0.80
Eu-Dy-MOF gel (1:1)	1:1	1:1.09
Tb-Dy-MOF gel (1:1)	1:1	1:1.21
Eu-Tb-Dy-MOF gel (1:1:1)	1:1:1	1:0.94:0.91

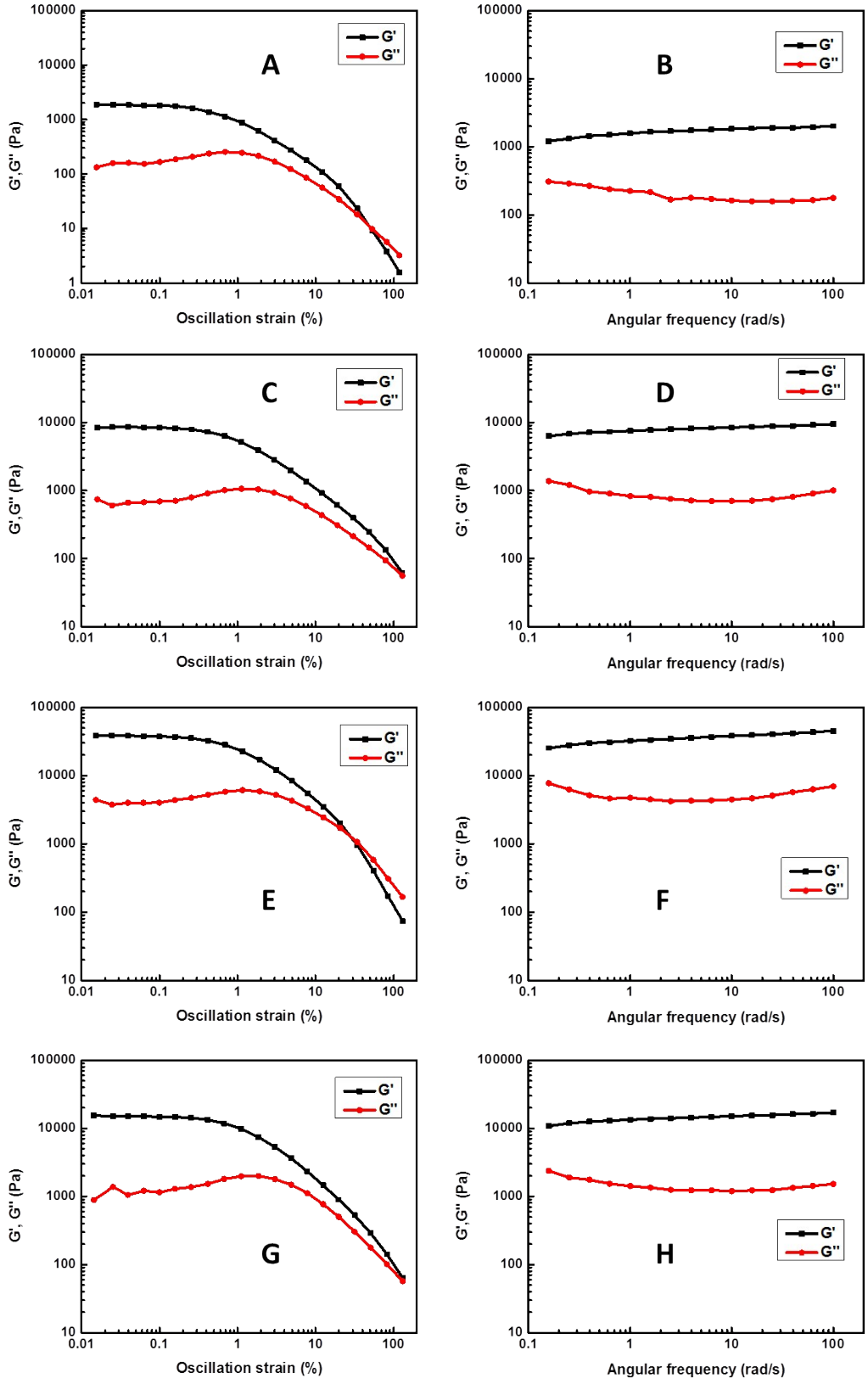

Figure S14. Viscoelastic properties of (A, B) Eu-Tb-MOF gels, (C, D) Eu-Dy-MOF gels, (E, F) Tb-Dy-MOF gels, and (G, H) Eu-Tb-Dy-MOF gels.

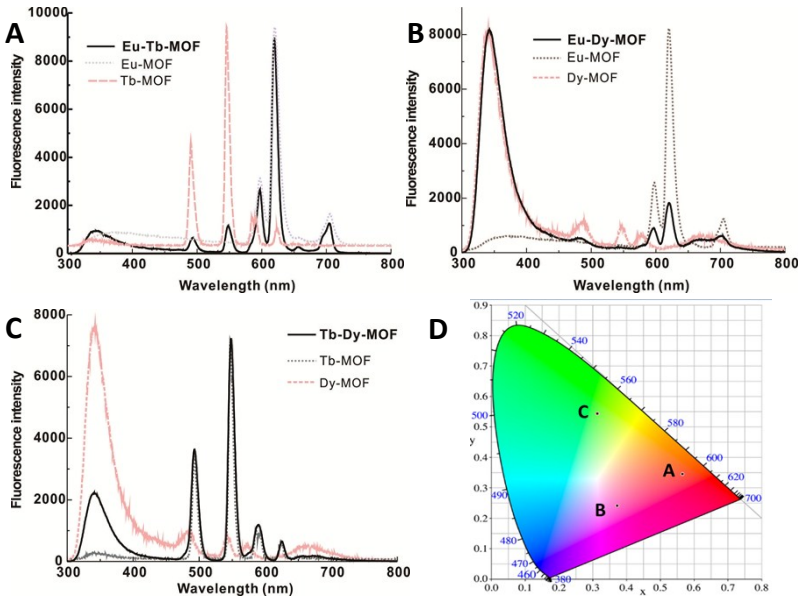

Figure S15. Fluorescence spectra of (A) Eu-Tb, (B) Eu-Dy, and (C) Tb-Dy MOF gels with the ratio of 1:1 under single-wavelength excitation at 275 nm. (D) CIE chromaticity coordinates of the emission from (A) Eu-Tb, (B) Eu-Dy, and (C) Tb-Dy MOF gels.

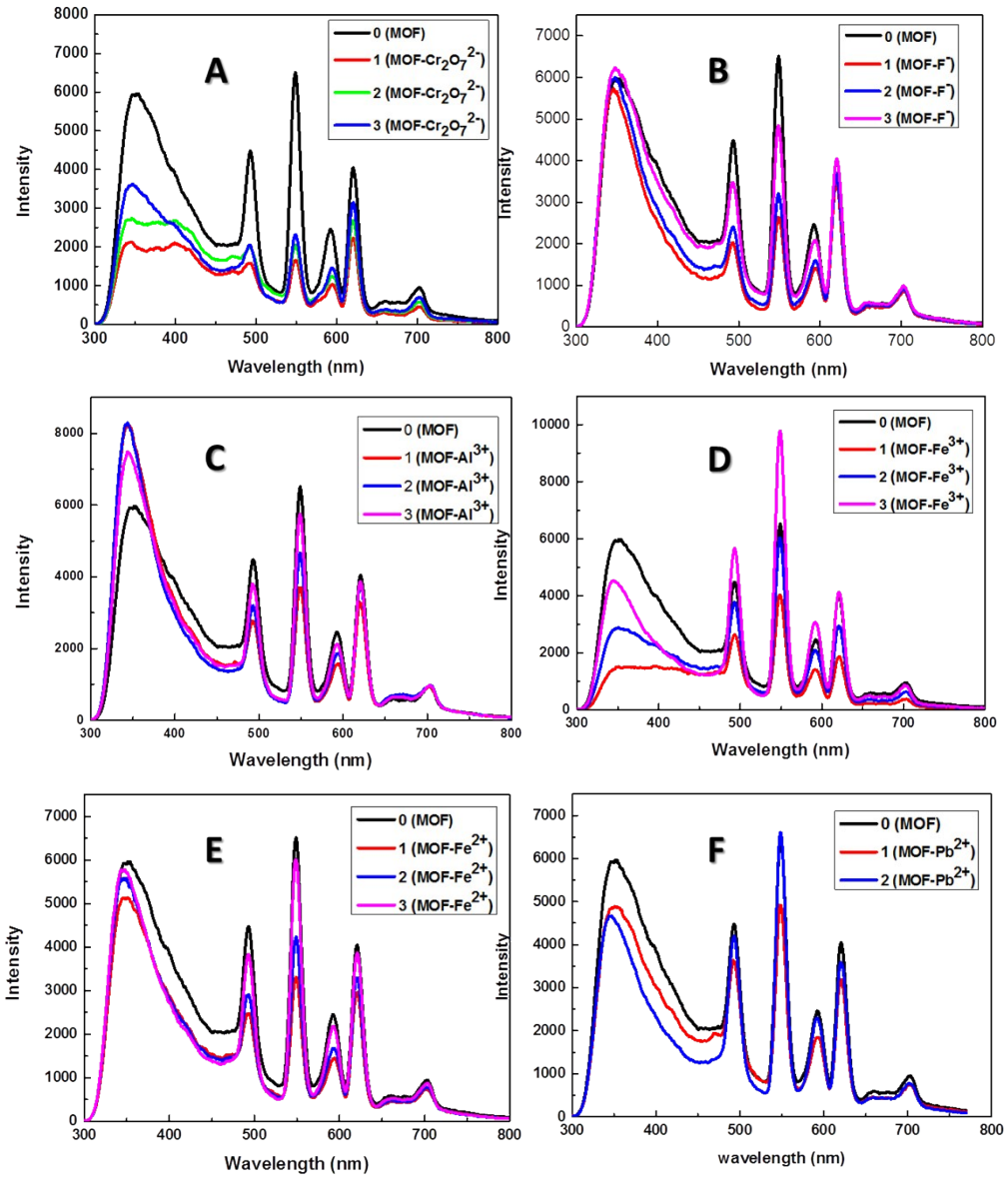

Figure S16. The fluorescence profiles of $Eu_{0.25}Tb_{0.25}Dy_{0.5}$-MOF gels after the addition of different targets. (A) $Cr_2O_7^{2-}$ ion, (B) F^- ions, (C) Al^{3+} ion, (D) Fe^{3+} ion, (E) Fe^{2+} ion, (F) Pb^{2+} ion at different concentrations under the excitation of 259 nm (1, 2, 3 represent the decreased concentrations).

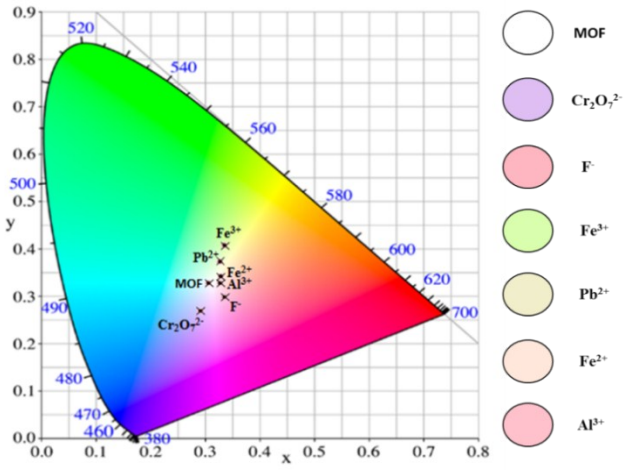

Figure S17. Multi-target fluorescence detection with single MOF gels under single excitation. The CIE coordinates for the response of Eu-Tb-Dy mixed-metal-MOF gels with the ratio of 1:1:2 in the precursors to different targets.

Fluorescence emission of white emitting MOF gel drastically decreased with increased $Cr_2O_7^{2-}$ concentration (Figure S13A). The presence of F^- reduced obviously the emission intensity of the Ln^{3+} in the MOF gels but slightly enhanced the intensity of 5-bop (Figure S13B). Al^{3+} ions weakened the fluorescence emission of the Ln^{3+} in the MOF gels but enhanced the emission of the ligand (Figure S13C). The fluorescence emission of the ligand decreased while the fluorescence emission of Ln^{3+} first decreased and then increased with the increasing of Fe^{3+} concentration (Figure S13D). Fe^{2+} ions quenched slightly the fluorescence emission of the ligand while the fluorescence emission of Ln^{3+} decreased gradually with the increasing of Fe^{2+} content (Figure S13E). The fluorescence emission of the mixed-metal MOF gels decreased gradually with increased Pb^{2+} concentration (Figure S13F).

The color changes of the white emitting MOF gels after addition of different species were illustrated in Figure S17. The existence of $Cr_2O_7^{2-}$ makes the color changed to be light purple, while the addition of F^- changed the emission to be pink, Fe^{3+} to be green, Fe^{2+} to be light yellow, Pb^{2+} to be light yellow green, and Al^{3+} to be light pink. Different emission was observed to reveal the application for multi-target fluorescence detection with the single white emitting MOF gels at single-wavelength excitation. Our system has higher integration degree and simpler sensing procedure than the previous multi-target detection ones.